

## Three Different Gating Models for Inactivation of the $I_{to}$ in Ventricular Myocytes of Rats and Mice

Z. CSERESNYÉS, Z. RUSZNÁK, A. BOZSÁNYI, J. MAGYAR, G. SZÜCS  
and L. KOVÁCS

*Department of Physiology, Medical University School of Debrecen,  
P.O.Box 22, H-4012 Debrecen, Hungary*

**Abstract.** Kinetic models to describe the time course of the  $\text{Ca}^{2+}$ -independent outward potassium current ( $I_{to}$ ) in cardiac ventricular cells were constructed. The  $I_{to}$  traces were recorded from isolated myocytes of rats and mice using the whole-cell configuration of the patch-clamp technique. An iterative method was developed to eliminate the capacitive transient overlapping the early part of the  $I_{to}$ . The isolated  $I_{to}$  curves were then fitted by Hodgkin-Huxley type functions and different inactivation gating mechanisms were identified in various groups of the animals. In some Wistar rats a single inactivation route was found. Another group of Wistar rats and diabetic BB/Mol rats showed two independent inactivation pathways both of which resulted in a completely closed channel. In lean specimen of C-57 mice and in streptozotocin-treated Wistar rats the two inactivation gates gave closed channels only when both parallel inactivating transitions have been completed. In this case a possible interaction between the gating particles has been revealed.

**Key words:** Hodgkin-Huxley equations — Kinetic analysis — Capacitive transient — Model identification — Transient outward potassium current

### Introduction

The transient outward potassium current ( $I_{to}$ ) plays a significant role in the determination of the action potential configuration in the cardiomyocytes of different species (Josephson et al. 1984). Consequently, the heterogeneity in the time course of the action potential seen under physiological circumstances can be partly interpreted as a result of the variability in the  $I_{to}$  characteristics (Bénitah et al. 1993). Moreover, several authors have described the sensitivity of the  $I_{to}$  to various patho-

---

Correspondence to: Zoltán Cseresnyés, Department of Biological Chemistry, University of Maryland Medical School, 108 N. Greene Street, Room 229, Baltimore, MD 21201 USA

logical conditions as well (Magyar et al 1992, Shimom et al 1992 Jourdon and Feuvray 1993) Despite the significance of this current, our knowledge about its kinetic behaviour, gating mechanism and pharmacological sensitivity is still limited, mainly because the recording of a single  $I_{to}$  channel activity is difficult

When studying the ionic mechanisms responsible for the electrophysiological changes in various diabetic models the kinetic features of the  $I_{to}$  were found to vary in a rather wide range To describe the kinetic characteristics a Hodgkin Huxley type (HH) characterization of the  $I_{to}$  records seemed reasonable since the transitions between the open closed and inactive states of the channels can be properly approximated by this method (Beaumont et al 1993a b)

A serious methodological problem during the analysis arises from the rapid activation of the  $I_{to}$  Namely when using the whole-cell configuration of the patch clamp technique the capacitive transient overlaps the rising phase of the  $I_{to}$ , making the fitting procedure difficult Several techniques have been described to eliminate the capacitive transient (i.e. analogue compensation linear extrapolation and subtraction etc.) but all of these approaches have certain disadvantages

In this paper we introduce a technique which allows an accurate approximation of the activation of the  $I_{to}$  Moreover we employ an HH characterization to describe three distinct gating mechanisms for the calcium independent outward potassium currents in ventricular cardiomyocytes isolated from different types of rats and mice

## Materials and Methods

### *Animals*

*Wistar rats* Six animals of both sexes were used aged 12 weeks with 150–200 g body weight *Streptozotocin treated Wistar rats (STZ rats)* Insulin dependent diabetes mellitus (Type I IDDM) was induced in six Wistar rats by a single intravenous dose of 51/6 mg/kg body weight (SIGMA) the blood glucose levels ranged between 17.6 and 27.7 mmol/l *BB/Mol rats* Four genetically diabetic (IDDM) BB/Mol rats of both sexes purchased from the Mollegaard Breeding Centre Ltd (Ejby Denmark) the PB/Wor Mol BB colony were used The animals were 12–24 weeks old and weighed 170–350 g at the time of the experiments Their blood glucose levels were held at 18–22 mmol/l (checked twice a week) with insulin administration (Ultralente Novo Industri AS Copenhagen 0.5–5 IU/day/animal depending on the body weight and the blood glucose level) *C57 type lean mice* Mice (4 animals) aged between 20–24 weeks at the time of the experiments their body weight varied between 20–25 g

### *Cell isolation*

The animals were killed with a blow on the neck The heart was then removed and perfused on a Langendorff column The cell isolation was performed in three steps using continuously oxygenated solutions with a temperature of 37°C In the first step the blood

was washed out from the heart with Tyrode's solution (in mmol/l: NaCl, 150.0; KCl, 5.4;  $MgCl_2$ , 0.5; HEPES, 5.0; glucose, 10.0; pH adjusted to 7.2 by NaOH) containing 1 mmol/l  $Ca^{2+}$ . In the second step nominally calcium-free Tyrode's solution was perfused for 5 minutes, and finally the enzyme-containing Tyrode's solution with 180  $\mu$ mol/l  $Ca^{2+}$  was applied for 30–50 minutes (8–10 mg collagenase/40 ml Tyrode's solution; SIGMA, Type 1). The heart was then chopped into small pieces, shaken in a test tube and the isolated ventricular myocytes were suspended in the storage solution (in mmol/l: KCl, 85.0;  $KH_2PO_4$ , 30.0;  $MgCl_2$ , 3.0; glucose, 10.0; K-glutamate, 16.0; EGTA, 0.5;  $KHCO_3$ , 3.0; pyruvic acid, 5.0; HEPES, 10.0; taurine, 20.0; pH set to 7.4 by KOH). The suspension was stored for 1–3 hours at +5°C before use. The measurements were performed on cells bathed in Tyrode's solution containing 2 mmol/l  $CaCl_2$ . In order to block calcium and sodium currents, 3 mmol/l  $CoCl_2$  and 20  $\mu$ mol/l tetrodotoxin (TTX) were applied into the external solution. All the chemicals were purchased from Reanal (Hungary) and from SIGMA (USA).

#### *Voltage-clamp experiments*

The whole-cell clamp configuration of the patch-clamp technique was employed (Hamill et al. 1981). The holding potential was  $-85$  mV throughout. In order to inactivate the TTX-insensitive sodium current, a prepulse to  $-20$  mV was applied with a duration of 7 ms. The 900 ms long test pulse changed the membrane potential between  $-100$  mV and  $+50$  mV in 10 mV steps. Only the current traces recorded between 0 mV and  $+50$  mV were used in the present work. In some cases extra long clamp pulses (2000 ms) were applied to check the existence of a very slowly inactivating component. The resistance of the microelectrodes was 3–5 MOhm when filled with the internal solution (in mmol/l: K-aspartate, 130.0; KCl, 20.0;  $KH_2PO_4$ , 1.0;  $MgCl_2$ , 1.0; EGTA, 5.0;  $Na_2$ -ATP, 3.0; HEPES, 5.0; pH adjusted to 7.3 by KOH). The Pyrex glass tubes for the microelectrodes were purchased from Clark Electromedical Instruments (UK).

#### *Data acquisition and analysis*

AXOPATCH-1D and AXOPATCH-200 amplifiers (Axon Instruments, Foster City, CA) were employed in the experiments. Four-pole low-pass Bessel filters were used with a corner-frequency of 2 kHz. Pulse formation and data acquisition were performed by IBM PCs equipped with Labmaster TM 40-type 12 bit AD/DA converters (Scientific Solutions, Foster City, CA). The converters were controlled by the pCLAMP 5.5.1 software (Axon Instruments, Foster City, CA).

Data analysis was completely done with a home-made software written in Borland PASCAL 6.0 for Windows. The analogue current records were leakage corrected trace-by-trace. The first point of the fitting range was defined as the peak value of the capacitive current transient while the final point was set at 900 ms. Two methods were applied to eliminate the shading effect of the capacitive transient. A method introduced by Benndorf and Nilius (Benndorf and Nilius 1988; hereinafter referred to as Truncated Method, TM) neglected the first 2/3 of the activation part of the analogue trace and the remaining part was used for fitting. Moreover, to fit the activation of the current traces more properly, a new method (see Results) was developed (Iterative Method, IM).

Weighted averages were calculated during the data analysis. The error bars represent weighted deviation unless the scatter is smaller than the symbol.

## Results

### *An iterative method to eliminate the shading effect of the capacitive transient*

The difficulties caused by the capacitive current when fitting the raising part of the current traces were eliminated by an iterative procedure. The fitting algorithm was the  $\chi^2$  minimizing Nelder-Mead simplex method.

In the first step of the iteration, the leakage corrected analogue current trace was fitted by the sum of a single exponential (capacitive transient; Eq. 1) and an appropriate HH function (Eq. 8,9 or 21). The capacitive transient reconstructed from the fitted parameters was then subtracted from the original record point-by-point. The difference current trace was fitted by the HH function, the obtained parameters were used to construct the potassium current which was subtracted from the original record, leaving the isolated capacitive transient. This was then fitted by the function:

$$I_c = I_c^{\max} \cdot e^{-\frac{t}{\tau_c}} \quad (1)$$

where  $I_c$  is the capacitive current at time  $t$ ;  $I_c^{\max}$  is the maximum value of the capacitive transient; and  $\tau_c$  is the time constant.

The capacitive transient was reconstructed again and subtracted from the original trace, providing the second approximation of the pure potassium current. The last two steps were repeated until convergence was reached. The convergence criterion was to have changes less than 5% in any of the fitted parameters compared to the values in the preceding iteration. To improve the quality of the fit in the first 30–50 ms of the traces, a weighting factor was introduced when calculating the  $\chi^2$  values of the data points in this range. The decay phase of the capacitive transient and the raising phase of the potassium current up to the peak were weighted by 10 while the valley between them by 20. The iterative method is illustrated in Fig. 1a where the original potassium current transient, the calculated potassium current and the calculated capacitive transient are plotted after final convergence.

The parameter values given by the IM and TM for the same current trace showed systematic differences. The activation time constant ( $\tau_1$ ) was usually underestimated and the rate constant of the closed-to-open transition ( $\alpha$ ) was overestimated by the TM. The shorter the time-to-peak and the higher the capacitive transient, the more definite this difference (e.g. BB/Mol rats, Fig. 1b). A similar difference, however, was not present in lean mice, which were characterized by bigger time-to-peak and smaller  $\tau_c$  values (Fig. 1c).

### *Model with a single inactivation state*

The original solution of the HH differential equations (Hodgkin and Huxley 1952) was given for the potassium and the sodium currents of the squid giant axon. For the sodium channels one inactivation step was supposed, which could be described

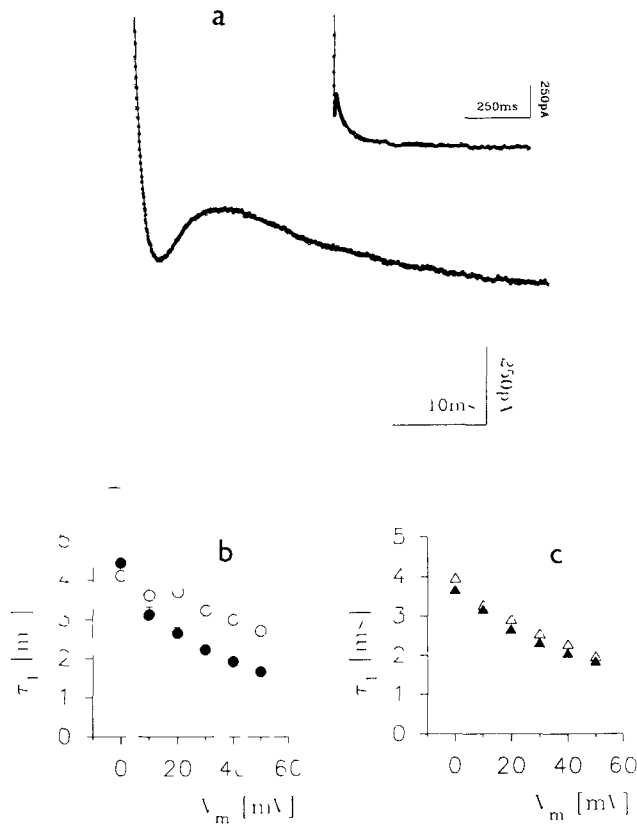
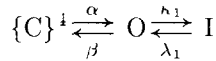


**Figure 1.** Approximation of the activation kinetics of the transient outward potassium current (A) The Iterative Method (IM) was used to fit the current record obtained at +30 mV in a ventricular myocyte of a BB/Mol rat using Eqs 1 and 9. The calculated capacitive current (dotted line) the calculated pure potassium current (dashed line) and their sum (full line) are shown together with the analogue trace (circles). To illustrate the reliability of the fit the total currents are plotted on two different time bases. The horizontal broken lines indicate the zero current level. The  $\tau_1$  activation time constant values obtained by Eq 9 are plotted in the function of the membrane potential for BB/Mol rats (B,  $n = 5$ ) and for lean mice (C,  $n = 9$ , obtained by Eq 21). The values provided by the truncated method and by the iterative method are represented with filled and open symbols, respectively.

by a single exponential decay function. A similar gating model for the  $I_{to}$  can be Scheme 1



Scheme 1

Throughout this paper,  $\alpha$  and  $\beta$  indicate the transitional rates between the closed and open states,  $\kappa_1$  and  $\lambda_1$  mark those between open and inactivated positions. When there are two inactivated states, the subscripts of  $\kappa$  and  $\lambda$  refer to the transitional rates of the appropriate inactivation pathways. The C-O transitional rate constants can be calculated using the equations

$$\alpha = \frac{p_\infty}{\tau_1} \quad (2)$$

$$\beta = \frac{1 - p_\infty}{\tau_1} \quad (3)$$

where  $\tau_1$  is the activation time constant,  $1 - p_\infty$  gives the ratio of the gating particles in the activated state at the end of the pulse ( $t \rightarrow \infty$ ).  $p_\infty$  can be calculated by the equation:

$$p_\infty = \left( \frac{A(V)}{A(V_{\max})} \cdot \frac{V_{\max} - V_r}{V - V_r} \right)^{\frac{1}{4}} \quad (4)$$

where  $V_r$  is the resting membrane potential (taken as  $-85$  mV),  $V$  is the actual membrane potential,  $V_{\max}$  is the membrane potential at maximum depolarization ( $+50$  mV), and  $A$  is the fitted maximum current amplitude at the given membrane potential, supposing zero inactivation.

The O-I rate constants can be calculated by the equations

$$\lambda_1 = \frac{q_\infty}{\tau_2} \quad (5)$$

and

$$\kappa_1 = \frac{1 - q_\infty}{\tau_2} \quad (6)$$

where  $\tau_2$  is the inactivation time constant,  $1 - q_\infty$  is the ratio of gating units in the inactivated state at  $t \rightarrow \infty$ .

The incomplete inactivation of the current ( $\lambda > 0$ ) can be accounted for by incorporating the  $K$  pedestal parameter into the simplified HH equations (Benndorf and Nilius 1988). The pedestal parameter can be calculated as

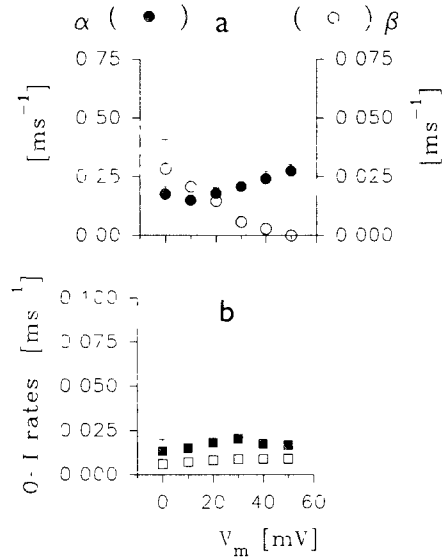
$$K \doteq \frac{q_\infty}{1 - q_\infty} \quad (7)$$

The fitting function used for the model with one inactivation state and with a non-zero steady-state current (supposing complete recovery from inactivation at the beginning of every voltage step) was:

$$I(t) = A \cdot \left(1 - e^{-\frac{t}{\tau_1}}\right)^4 \cdot \left(e^{-\frac{t}{\tau_2}} + K\right) \cdot \frac{1}{K + 1} \quad (8)$$

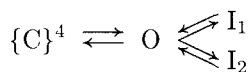
where  $I(t)$  is the potassium current at time  $t$  while the other symbols have the same definitions as previously.  $I_{to}$  traces recorded in a sub-group of Wistar rats (3 animals) could be described by this model. The transitional rate constants are shown in Fig. 2. The  $\alpha$  values were about one order of magnitude larger than the  $\beta$  rate constants,  $\alpha$  increased while  $\beta$  decreased at more positive membrane potentials. The  $\kappa_1$  rate constants were about two times larger than the  $\lambda_1$  values, these rate constants being voltage independent in the voltage range studied.

**Figure 2.** Rate constants obtained by the model with single inactivation state.  $I_{to}$  records from Wistar rats were fitted by Eqs. 1 and 8, the transitional rate constants were calculated using Eqs. 2-6, and their values were plotted as the function of the membrane potential. (a):  $\alpha$  (filled circles, left ordinate) and  $\beta$  (open circles, right ordinate) rate constants characterizing the C-O transitions. (b):  $\kappa_1$  (filled squares) and  $\lambda_1$  (open squares) rate constants describing the O-I transitions.



#### *A multiplicative model with two inactivated states*

In most cases the decay phase of the  $I_{to}$  current transients could not be fitted by Eq. 8. Consequently, we had to suppose at least two inactivated states. The multiplicative model supposes that each of the two inactivated states means complete closing of the channels:



**Scheme 2**

The function used to fit the current traces with this model can be derived from Eq. 8 by introducing a second inactivation term in multiplicative manner:

$$I(t) = A \cdot \left(1 - e^{-\frac{t}{\tau_1}}\right)^4 \cdot \left(e^{-\frac{t}{\tau_2}} + K\right) \cdot \frac{1}{K+1} \cdot \left(e^{-\frac{t}{\tau_3}} + L\right) \cdot \frac{1}{L+1} \quad (9)$$

where  $\tau_3$  is the second inactivation time constant. The second pedestal parameter

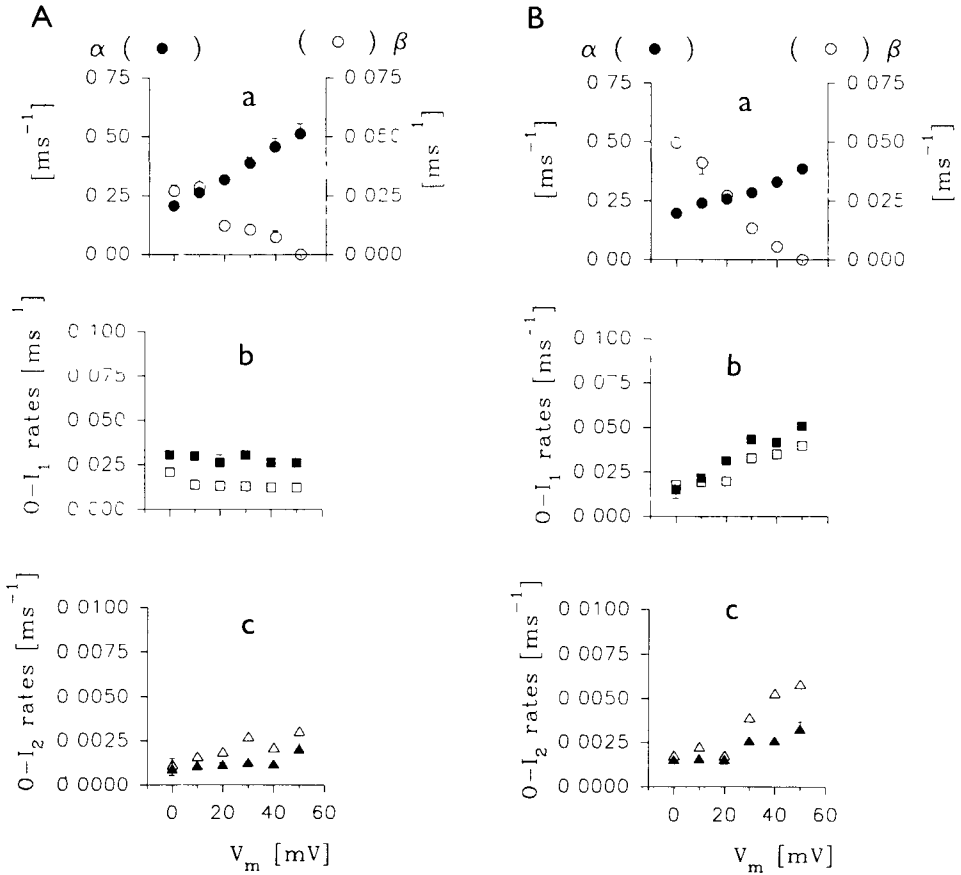


**Figure 3.** Rate constants obtained by the multiplicative model.  $I_{to}$  records measured in Wistar rats ( $n = 3$ ; part *A*) and in BB/Mol rats ( $n = 5$ ; part *B*) were fitted by Eqs. 1 and 9, the transitional rate constants were calculated using Eqs. 2-6 and 10, and their values were plotted as function of the membrane potential. Panels *a* show the  $\alpha$  (filled circles, left ordinate) and  $\beta$  (open circles, right ordinate) rate constants of the C-O transition. Panels *b*:  $\kappa_1$  (filled squares) and  $\lambda_1$  (open squares) rate constants of the O-I<sub>1</sub> transition. Panels *c*:  $\kappa_2$  (filled triangles) and  $\lambda_2$  (open triangles) rate constants of the O-I<sub>2</sub> transition.

$L$  is defined as

$$L \doteq \frac{r_\infty}{1 - r_\infty} \quad (10)$$

where  $1 - r_\infty$  is the ratio of the gating particles in the second inactivated state at  $t \rightarrow \infty$ . On the basis of the model identification (see below) the other subgroup of the Wistar rats (3 animals) and the BB/Mol rats could be characterized by this model. The transitional rate constants are shown in Fig. 3. The  $\alpha$  and  $\beta$  were voltage dependent,  $\alpha$  increased while  $\beta$  decreased with higher depolarizations. The  $\kappa_1$  and  $\lambda_1$  transition rates proved to be voltage independent in Wistar rats (Fig. 3A/b) while they increased at more positive voltages in BB/Mol rats (Fig. 3B/b). The  $\lambda_2$  values were slightly larger than  $\kappa_2$  (Fig. 3A/c and 3B/c), opposite to that obtained for all other  $\kappa$  and  $\lambda$  rate constants. Both  $\kappa_2$  and  $\lambda_2$  were voltage-independent in Wistar rats (Fig. 3A/c) but they increased at more positive membrane potentials in BB/Mol rats (Fig. 3B/c).

*An additive model with two inactivated states*

This model predicts closed channels (zero current) only if both of the two inactivating particles have moved. The different gating particles may belong to different channel populations (Huguenard et al. 1991) or may be located in the same channel providing two parallel inactivation routes. In the frame of this model the total current can be treated as the sum of two components. These components may flow through the two channel populations or the two currents can be defined on the basis whether they inactivate towards  $I_1$  or  $I_2$  state, respectively (both  $I_1$  and  $I_2$  have to have non-zero conductance now). The function used for fitting the current traces according to this model can be derived from Eq. 8 as the sum of the two current components:

$$I(t) = I_1(t) + I_2(t) \quad (11)$$

$$I_1(t) = A_1 \left(1 - e^{-\frac{t}{\tau_1}}\right)^4 \cdot \left(e^{-\frac{t}{\tau_2}} + K_1\right) \cdot \frac{1}{K_1 + 1} \quad (12)$$

$$I_2(t) = A_2 \cdot \left(1 - e^{-\frac{t}{\tau_1}}\right)^4 \cdot \left(e^{-\frac{t}{\tau_3}} + K_2\right) \cdot \frac{1}{K_2 + 1} \quad (13)$$

Substituting Eqs. 12–13 into Eq. 11 gives

$$I(t) = \left(1 - e^{-\frac{t}{\tau_1}}\right)^4 \cdot \left[ \left( A_1 \cdot e^{-\frac{t}{\tau_2}} + A_1 \cdot K_1 \right) \cdot \frac{1}{K_1 + 1} + \left( A_2 \cdot e^{-\frac{t}{\tau_3}} + A_2 \cdot K_2 \right) \cdot \frac{1}{K_2 + 1} \right] \quad (14)$$

and rearranging Eq. 14 results in

$$I(t) = \left(1 - e^{-\frac{t}{\tau_1}}\right)^4 \cdot \left[ \frac{A_1}{K_1 + 1} \cdot e^{-\frac{t}{\tau_2}} + \frac{A_1 \cdot K_1}{K_1 + 1} + \frac{A_2}{K_2 + 1} \cdot e^{-\frac{t}{\tau_3}} + \frac{A_2 \cdot K_2}{K_2 + 1} \right] \quad (15)$$

A factor which defines the share of the two components in the inactivation can be defined (marked as  $S$  hereinafter) if the multipliers of  $e^{-\frac{t}{\tau_2}}$  and  $e^{-\frac{t}{\tau_3}}$  are divided by the sum of these expressions (introducing as  $B$ ; Eq. 16) as it follows

$$B \doteq \frac{A_1}{K_1 + 1} + \frac{A_2}{K_2 + 1} \quad (16)$$

$$S \doteq \frac{A_1}{K_1 + 1} \cdot \frac{1}{B} \quad (17)$$

Eq. 15 can be rewritten as

$$I(t) = B \cdot \left(1 - e^{-\frac{t}{\tau_1}}\right)^4 \cdot \left[ S \cdot e^{-\frac{t}{\tau_2}} + (1 - S) \cdot e^{-\frac{t}{\tau_3}} + S \cdot K_1 + (1 - S) \cdot K_2 \right] \quad (18)$$

The time-independent terms can be combined into a pedestal parameter  $K$  as

$$K \doteq S \cdot K_1 + (1 - S) \cdot K_2 \quad (19)$$

The pedestal parameter  $K$  should appear as an additive term in the inactivation part and, at the same time, the expression  $1/(K + 1)$  should multiply the whole function. To achieve this a new amplitude value ( $A$ ) was introduced:

$$A \doteq (K + 1) \cdot B \quad (20)$$

Substituting Eqs. 19–20 into Eq. 18 the final form of the fitting function will be:

$$I(t) = A \cdot \left(1 - e^{-\frac{t}{\tau_1}}\right)^4 \cdot \left[ S \cdot e^{-\frac{t}{\tau_2}} + (1 - S) \cdot e^{-\frac{t}{\tau_3}} + K \right] \cdot \frac{1}{K + 1} \quad (21)$$

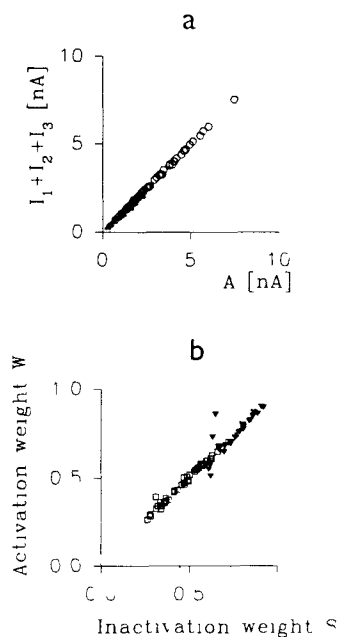
To prove that the share of the  $I_1(t)$  and  $I_2(t)$  current components (Eq. 11–13) from the total current can be calculated using the  $S$  factor, the falling phases of the  $I_{to}$  traces were fitted by the sum of two exponentials and a steady-state component as

$$I(t) = I_1 \cdot e^{-\frac{t}{\tau_2}} + I_2 \cdot e^{-\frac{t}{\tau_3}} + I_4 \quad (22)$$

where  $I_1$ ,  $I_2$  and  $I_4$  are the amplitudes of the current components of the falling phase extrapolated to  $t = 0$ ,  $\tau_2$  and  $\tau_3$  are the inactivation time constants provided by Eq. 21. Figure 4a shows that in every case the sums of  $I_1$ ,  $I_2$  and  $I_4$  values matched with the appropriate  $A$  parameters. The linear regression factor was 0.9891 for mice and 0.9206 for STZ rats. As a conclusion,  $I_1$  and  $I_2$  can be used instead of the unknown parameters  $A_1$  and  $A_2$ . In this case, the weight of the first current component in the total current can be determined as

$$W \doteq \frac{I_1}{I_1 + I_2} \quad (23)$$

**Figure 4.** The experimental background of Eqs 21 and 25. Panel *a*: The sum of the partial amplitudes  $I_1 + I_2 + I_3$  obtained by fitting the decay phase of the  $I_t$  using Eq 22 is plotted as the function of the theoretical maximum current amplitudes calculated by the additive model (Eq 21). Data for all cells and at all membrane potentials are plotted for mice (open circles) and STZ rats (filled triangles). The linear regression factor was 0.9891 and 0.9206 for lean mice and STZ rats respectively. Panel *b*: The weight factor ( $W$ ) characterizing the share of the two current components in the activation part (provided by Eq 23) is plotted as the function of parameter  $S$  (Eq 21). Data of all cells and at all membrane potentials are plotted for mice (open squares) and STZ rats (filled triangles). The linear regression coefficient was 0.9203 and 0.9363 for lean mice and STZ rats respectively.



where  $W$  stands for the weight of the first current component in the total current. In Fig. 4b the calculated  $W$  values are plotted against the appropriate fitted  $S$  parameters. The linear correlations were acceptable in both cases with regression factors of 0.9203 in mice and 0.9363 in STZ rats. Consequently, the share of the theoretical maximum amplitudes ( $A_1$  and  $A_2$ ) on the total  $I_t$ , can be calculated by the weight factor  $S$  in the following way:

$$A_1 = S \cdot A \quad (24)$$

$$A_2 = (1 - S) \cdot A \quad (25)$$

Substituting Eqs 24-25 into Eq 20:

$$A = (K + 1) \cdot A \cdot \left( \frac{S}{K_1 + 1} + \frac{1 - S}{K_2 + 1} \right) \quad (26)$$

Expressing  $K_2$  from Eq 19 as:

$$K_2 = \frac{K - S \cdot K_1}{1 - S} \quad (27)$$

and substituting it into Eq 26 the result for  $K_1$  is:

$$K_1 = K \quad (28)$$

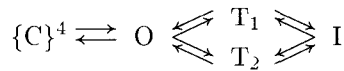
and the result for  $K_2$  using Eq. 27:

$$K_2 = K \quad (29)$$

Consequently,  $q_\infty$  and  $r_\infty$  are also equal:

$$q_\infty = r_\infty = \frac{K}{K+1} \quad (30)$$

As an important conclusion of this equality, the gating scheme should be re-drawn as follows:



**Scheme 3**

where  $T_1$  and  $T_2$  represent transitional states from where the channel likely goes to the final, single inactivated state  $I$  (in this model  $\kappa_1$ ,  $\lambda_1$ ,  $\kappa_2$  and  $\lambda_2$  rate constants illustrate the complex O-T-I transitions). The possible existence of the common inactivated state makes the interpretation of the  $I_{to}$  as the sum of two currents flowing through two independent channel populations unlikely.

The additive model was found the most appropriate to describe the inactivation kinetics of  $I_{to}$  in lean mice and STZ rats. The rate constants are shown in Fig. 5. The  $\alpha$  increased while the  $\beta$  decreased with the increasing depolarization. The  $\kappa$  and  $\lambda$  rate constants were voltage-independent in lean mice (Fig. 5A/b and c) while each of them increased with higher depolarization in STZ rats (Fig. 5B/b and c). The rate constants characteristic of the O-T<sub>1</sub>-I transition ( $\kappa_1$  and  $\lambda_1$ ) were about one order of magnitude larger than those describing the O-T<sub>2</sub>-I transition ( $\kappa_2$  and  $\lambda_2$ ).

#### *Model identification*

In a sub-group of Wistar rats the decay phase of the  $I_{to}$  could be fitted by Eq. 8 even when the current accompanied an extra long depolarizing pulse (2000 ms). Therefore, the application of the other models was not reasonable. The  $I_{to}$  transients of the other animals showed more complicated inactivation kinetics, they could be appropriately fitted only by the double exponential functions derived from the two complex gating models (Eq. 9 and Eq. 21).

When these functions were applied for a given trace, they gave very similar values for the  $R^2$  and  $\chi^2$ , therefore, their validity could not be decided upon the basis of these parameters. Distinction between the applicability of the multiplicative and additive models could be made by comparing the inactivation time constants (although also the time constants were rather similar). In some Wistar

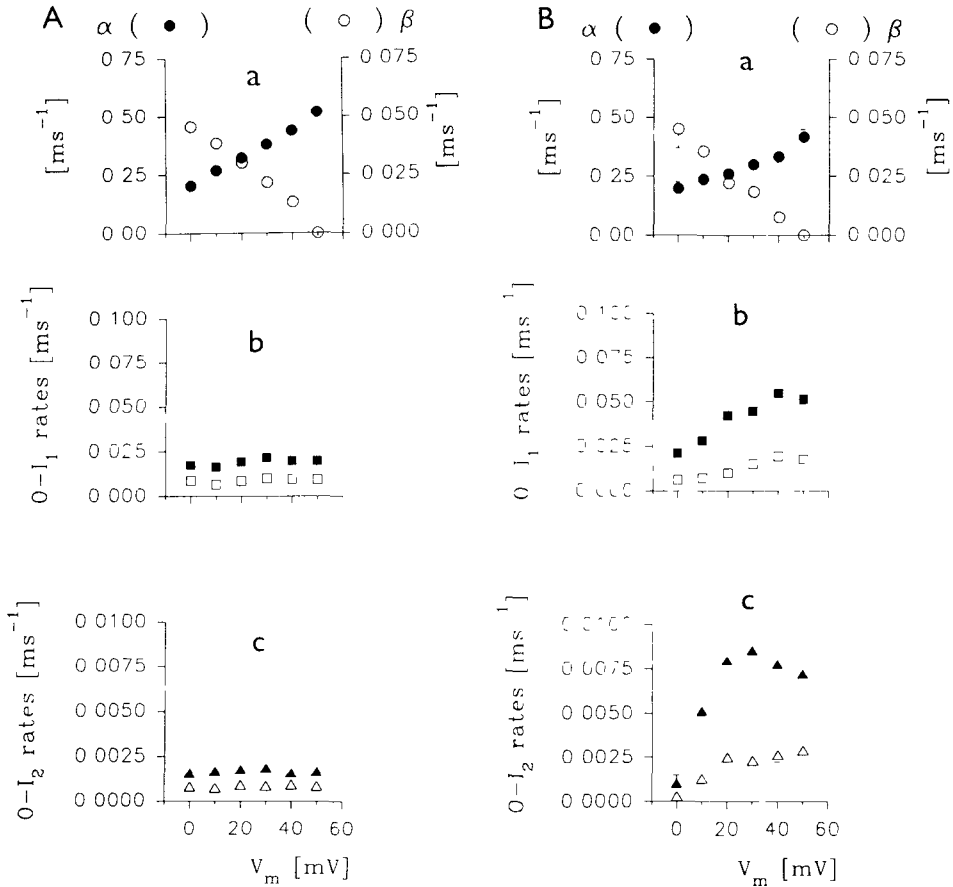


**Figure 5.** Rate constants obtained by the additive model.  $I_{T_0}$  transients recorded in lean mice ( $n = 9$ ; part *A*) as well as in STZ rats ( $n = 6$ ; part *B*) were fitted by Eqs. 1 and 21. the transitional rate constants were calculated using Eqs. 2–6, 10 and 28–30, their values plotted as function of the membrane potential. Panels *a* show the  $\alpha$  (filled circles, left ordinate) and  $\beta$  (open circles, right ordinate) rate constants of the C-O transition. Panels *b*:  $\kappa_1$  (filled squares) and  $\lambda_1$  (open squares) rate constants of the O-T<sub>1</sub>-I transition. Panels *c*:  $\kappa_2$  (filled triangles) and  $\lambda_2$  (open triangles) rate constants of the O-T<sub>2</sub>-I transition.

rats and in the BB/Mol rats, both models provided the same  $\tau_2$  and  $\tau_3$  values (including the equality of their standard deviations). In the STZ rats and lean mice this congruity was not perfect, the difference being mainly explicit at smaller depolarizations (between 0 and +30 mV) for both the  $\tau_2$  and the  $\tau_3$  values.

An explanation for the above behavior of the inactivation time constants can

be obtained by the fact that the additive model predicts closed channel if both of the inactivation particles are in their inactivating positions, while in the multiplicative model complete inactivation can already be reached when only one of the gating particles moved into its inactivating state. If a certain  $I_{to}$  trace reflects additive gating, fitting by Eq. 21 perfectly describes the O-T-I routes, but the fitting by the multiplicative model function (Eq. 9) cannot characterize the two different inactivating pathways: consequently, the inactivation time constants given by the two methods will be different. On the other hand, if a current trace inactivates according to the multiplicative model, the time constants predicted by the two methods should prove to be equal. Namely, in this case the additive gating mechanism will behave as if the  $T_1$  and  $T_2$  particles moved together to their inactivating positions, and the models are no longer distinctive in terms of the whole-cell measurements.

However, these two gating mechanisms are still distinct. The multiplicative model is based on assuming three independent events ( $p^1$ ,  $q$  and  $r$ ) and the joint probability can be given as the product of these three terms ( $p^1qr$ ), which is proportional to the current flowing through the channels. In the additive model, as the  $p^1(q+r)$  form of the fitting function indicates, the independence is supposed for the opening of the channels but not for the steps of the inactivation. The time dependence of the  $p$ ,  $q$  and  $r$  parameters were described by the classical HH equations but the application of the additive model has some significance beyond the HH theory itself. The similarity between the  $\tau_2$  and  $\tau_3$  values provided by the multiplicative and the additive models opens the possibility of a co-operative effect between the  $T_1$  and  $T_2$  particles. Consequently, if the  $T_1$  particle is the first to move towards its inactivating state, it drags the  $T_2$  gating unit of the same channel. Naturally, if  $T_2$  starts earlier, it pulls the  $T_1$  particle as well.

## Discussion

### *The reliability of the HH theory*

The first complete kinetic description of the sodium and potassium currents given by Hodgkin and Huxley in squid giant axon (Hodgkin and Huxley 1952) has been followed by many applications, modifications and re-investigations (e.g. Awiszus 1992; Bedrov et al. 1992; Kepler et al., 1992). Recent theoretical considerations have proven that the HH parameters can be successfully estimated when the peak current and the activation as well as the inactivation time constants are known and the time constant of activation is much smaller than that of inactivation (Meunier 1992; Beaumont et al. 1993a,b). Comparisons of the HH model with the linear analysis (Fishman et al. 1983; Fishman and Lipicky 1991) and with the Markov model (Chay 1988, 1991) also showed a good applicability of the HH theory al-

though the transitions between the closed and the inactivated states could not be characterized using the HH formalism.

#### *Description of the transient potassium currents*

The validity of the  $p^4q$  model in the fitting of the transient outward potassium currents has been confirmed by several studies (Benndorf and Nilius 1988; Huguenard et al. 1991; Mlinar and Enyeart 1993); consequently, we did not put emphasis on finding a better value for the power of  $p$ . The possible voltage dependence of the “ $p$ ” value was also disregarded, especially because we did not find any indications of the voltage dependence of the quality of the fitting of the rising phase.

Our attempts to fit the total outward potassium currents with the sum of a transient component (Eq. 8, supposing  $K = 0$ ) and a delayed rectifier type single exponential function (Apkon and Nerbonne 1991) were unsuccessful. The fact that the fitting of the A-current in neurons was performed as the sum of two transient current components with a common activation step (Huguenard et al. 1991) made reasonable to look for complex gating of the  $I_{t_o}$  channels supposing multiple inactivation routes.

#### *Elimination of the capacitive current transient*

The complete HH characterization of a given current requires the appropriate fitting of the raising phase as well as the decay of the analogue traces. In the case of rapidly activating currents such as the  $I_{t_o}$ , the capacitive transient at the beginning of the test pulse always remarkably hinders the approximation of the activation time course. The elimination of the capacitive transient can be performed by a built-in capacitance compensation of the patch-clamp amplifier. The main problem arising from this procedure is that the compensation circuit shows certain non-linearity. Moreover, the compensation usually cannot be complete in cardiomyocytes due to their high whole-cell capacitance ( $> 100$  pF; Magyar et al. 1992; Campbell et al. 1993a).

Another approach can be the determination of the capacitive transient by a voltage step of 5 mV (Bezanilla and Armstrong 1977; Coulter et al. 1989; Campbell et al. 1993a). The nonlinearity of the electrical properties of the membrane, however, makes the subtraction of the extrapolated capacitive transients from the current traces unreliable.

The separation of the  $I_{t_o}$  as a 4-aminopyridine (4-AP) sensitive component also seems reasonable (Apkon and Nerbonne 1991). Unfortunately, this technique usually causes a subtraction artefact (Bénitah et al. 1993) and the gating mechanism is affected by the drug (Castle and Slawsky 1992; Campbell et al. 1993b).

The TM (Benndorf and Nilius 1988) provides a reliable approximation for the activation and the inactivation time constants but it cannot overcome completely

the shading effect of the capacitive transient. Evident drawbacks of this method are a slight overestimation of the maximum current amplitude as well as an underestimation of the time-to-peak values and the activation time constants. The IM introduced in this paper allowed a correct description of both the capacitive and the outward potassium current components.

### *Kinetic models of the $I_{to}$*

The total outward potassium currents have usually been characterized by two inactivation time constants while the 4-AP sensitive  $I_{to}$  was found to have single exponential decay (Apkou and Nerbonne 1991; Magyar et al. 1992; Bénitah et al. 1993). In the present work the single exponential fit of the decay phase proved to be appropriate for the total current in a sub-group of Wistar rats, while other animals of the same strain showed complex inactivation. A possible explanation of this finding may be the heterogeneity of the transient outward current. It has been shown recently that both the functional channel densities and the inactivation kinetics of  $I_{to}$  were different in cells isolated from various parts of the rat myocardium (Bénitah et al. 1993).

The voltage dependence of the C-O transitional rates in the single inactivation state model is similar to that shown by Hodgkin and Huxley (1952) for sodium channels while the numerical values of the rate constants were close to those given by Bénitah et al. (1993). The  $\lambda_1$  was not considerably smaller than  $\kappa_1$  which may explain the notable sustained current component.

Some other Wistar rats and the BB/Mol rats exhibited  $I_{to}$  channels which inactivated accordingly to the multiplicative model. The  $\alpha$  activation rate constant was smaller in BB animals than in Wistar rats. The  $\lambda_2$  was bigger than  $\kappa_2$  suggesting that the  $I_2$  state becomes unstable at more positive membrane potentials, and most of the channels inactivate through the O- $I_1$  route.

In STZ rats and lean mice the  $\tau_2$  and  $\tau_3$  values (mainly between 0 mV and +30 mV membrane potentials) differed significantly when fitted by the two complex models; consequently, in these animals the  $I_{to}$  channels seem to inactivate according to the additive model. Like in the previous models, the  $\tau_1$  parameter was model-independent, its values ranged between 2 and 4 ms. The activation time constants described by Benndorf and Nilius (1988) in mice were considerably smaller (0.8–1.2 ms). A possible explanation of this difference may be the use of different strains of mice in experiments and/or underestimation of  $\tau_1$  by the TM. The  $\alpha$  and  $\beta$  parameter values were very similar to each other and to those calculated for Wistar rats using the single exponential model. The differences between the  $\kappa$  and  $\lambda$  values are more pronounced in STZ rats than in lean mice. This fact is in good accordance with the experimental finding that the sustained component of the outward potassium current is more explicit in mice. The larger difference may

also indicate that the cooperativity between the inactivation particles is stronger in STZ rats than in lean mice

**Acknowledgements.** The authors are indebted to professor T Kovacs for providing the lean mice, to I Sipos for taking part in the experiments, and to Mrs A Molnar for technical assistance. This work was partly supported by grants from the Hungarian Science Foundation (OTKA 1453) and from the Hungarian Ministry of Welfare (ETT T-473/90)

## References

- Apkon M, Nerbonne J M (1991) Characterization of two distinct depolarization-activated  $K^+$  currents in isolated adult rat ventricular myocytes. *J Gen Physiol* **97**, 973–1011
- Awiszus F (1992) Reduction of a Hodgkin-Huxley type model for a mammalian neuron at body temperature. *Biol Cybern* **67**, 427–432
- Beaumont J, Robeige F A, Leon L J (1993a) On the interpretation of voltage-clamp data using the Hodgkin-Huxley model. *Math Biosci* **115**, 65–101
- Beaumont J, Robeige F A, Lemieux D R (1993b) Estimation of the steady-state characterization of the Hodgkin-Huxley model from voltage-clamp data. *Math Biosci* **115**, 115–186
- Bedrov Y A, Akoev G N, Dick O E (1992) Partition of the Hodgkin-Huxley type model parameter space into the regions of qualitatively different solutions. *Biol Cybern* **66**, 13–418
- Bentah J P, Gomez A M, Bailly P, daPonte J-P, Berson G, Delgado C, Lorente P (1993) Heterogeneity of the early outward current in ventricular cells isolated from normal and hypertrophied rat hearts. *J Physiol (London)* **469**, 111–138
- Beardorf K, Nilius B (1988) Properties of an early outward current in single cells of the mouse ventricle. *Gen Physiol Biophys* **7**, 449–466
- Bezanilla F, Armstrong C M (1977) Inactivation of the sodium channel. I. Sodium current experiments. *J Gen Physiol* **70**, 549–566
- Campbell D L, Rasmusson R L, Qu Y, Strauss H C (1993a) The calcium-independent transient outward potassium current in isolated ferret right ventricular myocytes. I. Basic characterization and kinetic analysis. *J Gen Physiol* **101**, 571–601
- Campbell D L, Qu Y, Rasmusson R L, Strauss H C (1993b) The calcium-independent transient outward potassium current in isolated ferret right ventricular myocytes. II. Closed state reverse use-dependent block by 4-aminopyridine. *J Gen Physiol* **101**, 603–626
- Castle N A, Slawsky M T (1992) Characterization of 4-aminopyridine block of the transient outward  $K^+$  current in adult rat ventricular myocytes. *J Pharmacol Exp Ther* **264**, 1450–1459
- Chay T R (1988) Kinetic modelling for the channel gating process from single channel patch clamp data. *J Theor Biol* **132**, 449–468
- Chay T R (1991) The Hodgkin-Huxley  $Na^+$  channel model versus the five-state Markovian model. *Biopolymers* **31**, 1483–1502
- Coulter D A, Huguenard J R, Prince D A (1989) Calcium currents in rat thalamocortical relay neurons: kinetic properties of the transient, low-threshold current. *J Physiol (London)* **414**, 587–604

- Fishman H. M., Lipicky R. J. (1991): Determination of  $K^+$ -channel relaxation times in squid axon membrane of Hodgkin-Huxley and by direct linear analysis. *Biophys. Chem.* **39**, 177—190
- Fishman H. M., Leuchtag H. R., Moore L. E. (1983): Fluctuation and linear analysis of Na-current kinetics in squid axon. *Biophys. J.* **43**, 293—307
- Hamill O. P., Marty A., Neher E., Sakmann B., Sigworth F. J. (1981): Improved patch-clamp techniques for high-resolution current recording from cells and cell-free membrane patches. *Pflügers Arch.* **391**, 85—100
- Hodgkin A. L., Huxley A. F. (1952): A quantitative description of membrane currents and its application to conduction and excitation in nerve. *J. Physiol.* **177**, 500—511
- Huguenard J. R., Coulter D. A., Prince D. A. (1991): A fast transient potassium current in thalamic relay neurones: kinetics of activation and inactivation. *J. Neurophysiol.* **66**, 1304—1315
- Josephson I. R., Sanches-Chapula J., Brown A. M. (1984): Early outward current in rat single ventricular cells. *Circ. Res.* **54**, 157—162
- Jourdon P., Feuvray D. (1993): Calcium and potassium currents in ventricular myocytes isolated from diabetic rats. *J. Physiol.* **470**, 411—429
- Kepler T. B., Abbott L. F., Marder E. (1992): Reduction of conductance-based neuron models. *Biol. Cybern.* **66**, 381—387
- Magyar J., Rusznák Z., Szentesi P., Szücs G., Kovács L. (1992): Action potentials and potassium currents in rat ventricular muscle during experimental diabetes. *J. Mol. Cell. Cardiol.* **24**, 841—853
- Meunier C. (1992): Two and three dimensional reductions of the Hodgkin-Huxley system: separation of time scales and bifurcation schemes. *Biol. Cybern.* **67**, 461—468
- Mlinar B., Enyeart J. J. (1993): Voltage-gated transient currents in bovine adrenal fasciculata cells. II. A-type  $K^+$  current. *J. Gen. Physiol.* **102**, 239—255
- Shimoni Y., Banno H., Clark R. B. (1992): Hyperthyroidism selectively modified a transient potassium current in rabbit ventricular and atrial myocytes. *J. Physiol.* **457**, 369—389

Final version accepted July 17, 1995